GEOPHYSICS, VOL. 75, NO. 5 (SEPTEMBER-OCTOBER 2010); P. 75A129–75A137, 7 FIGS.
10.1190/1.3477966

Petroleum reservoir characterization using downhole microseismic monitoring

S. C. Maxwell[1], J. Rutledge[2], R. Jones[3], and M. Fehler[4]

ABSTRACT

Imaging of microseismic data is the process by which we use information about the source locations, timing, and mechanisms of the induced seismic events to make inferences about the structure of a petroleum reservoir or the changes that accompany injections into or production from the reservoir. A few key projects were instrumental in the development of downhole microseismic imaging. Most recent microseismic projects involve imaging hydraulic-fracture stimulations, which has grown into a widespread fracture diagnostic technology. This growth in the application of the technology is attributed to the success of imaging the fracture complexity of the Barnett Shale in the Fort Worth basin, Texas, and the commercial value of the information obtained to improve completions and ultimately production in the field. The use of commercial imaging in the Barnett is traced back to earlier investigations to prove the technology with the Cotton Valley imaging project and earlier experiments at the M-Site in the Piceance basin, Colorado. Perhaps the earliest example of microseismic imaging using data from downhole recording was a hydraulic fracture monitored in 1974, also in the Piceance basin. However, early work is also documented where investigators focused on identifying microseismic trace characteristics without attempting to locate the microseismic sources. Applications of microseismic reservoir monitoring can be tracked from current steam-injection imaging, deformation associated with reservoir compaction in the Yibal field in Oman and the Ekofisk and Valhall fields in the North Sea, and production-induced activity in Kentucky, U.S.A.

INTRODUCTION

Microseismic imaging has developed into a common technique to image fracture-network deformation that accompanies oil and gas operations. The most extensive application of microseismic monitoring is to image hydraulic-fracture operations, although the technique is also used to monitor microseismic events induced by inelastic deformation associated with injection of steam/water/gas for secondary recovery and production (e.g., Maxwell and Urbancic, 2001). Associated with the growth of the technology have been several workshops and forums focused on the technology as well as dedicated sessions at AAPG, SPE, SEG, and EAGE conferences. The technology is somewhat unique in that although it is a geophysical method, its users and main drivers tend to be reservoir engineers. In fact, based on a keyword search on the respective Web sites, there is more discussion of the technology through SPE than with SEG and EAGE combined.

Although the routine application of microseismic monitoring is relatively new to the oil and gas industry, it has been used in geothermal fields since the 1970s and 1980s as a routine method to image fracture networks activated during production and injection (Majer and McEvilly, 1979; Denlinger and Bufe, 1982; Eberhart-Phillips and Oppenheimer, 1984) and during hydraulic-fracture stimulation (Albright and Hanold, 1976; Pearson, 1981; Pine and Batchelor, 1984; Fehler, 1989). Prior to observations of microseismicity associated with reservoir stimulation and monitoring, passive monitoring of microseismicity was used extensively in the mining industry to monitor stress changes around mine openings, primarily from the workplace hazard associated with induced seismicity (e.g., Gibowicz and Kijko, 1994). Microseismic monitoring has also been extensively studied as a technique to monitor crack development around underground excavations intended as sites for waste disposal (e.g., Collins and Young, 2000).

Manuscript received by the Editor 8 December 2009; revised manuscript received 3 April 2010; published online 14 September 2010.
[1]Schlumberger, Hydraulic Fracture Monitoring, Calgary, Alberta, Canada. E-mail: smaxwell@slb.com.
[2]Los Alamos National Laboratory, Geophysics Group, Los Alamos, New Mexico, U.S.A. E-mail: jrutledge@lanl.gov.
[3]Schlumberger Cambridge Research, Cambridge, U.K. E-mail: rjones23@slb.com.
[4]Massachusetts Institute of Technology, Department of Earth, Atmospheric, and Planetary Sciences, Cambridge, Massachusetts, U.S.A. E-mail: fehler@mit.edu.

Historically, the earliest passive seismic monitoring application during injection in a petroleum field is often considered to be the Rangely experiments, where a controlled injection was used to prove the occurrence of induced seismicity (Rayleigh et al., 1976). However, induced seismicity (earthquakes caused by anthropogenic activity) and triggered seismicity (earthquakes whose timing is caused by anthropogenic activity) have a history in oil and gas related to certain fields where felt seismicity reported by the public has been attributed to petroleum production (see Suckale 2010 for a comprehensive review). Relatively few petroleum fields experience significant earthquakes; much more common are numerous smaller events, or microseismicity. There is no uniform definition of microseismic event or microearthquake, so here we use the term to describe seismic events with a moment magnitude less than zero. The occurrence of microseismic events approximately follows earthquake frequency-magnitude statistics, such that for each decrease in magnitude unit, there is a 10–100 times increase in the number of smaller-magnitude events (Fehler and Phillips, 1991). This makes microseismicity much more ubiquitous than seismicity large enough to be felt or detected on the surface, and monitoring these small-magnitude microearthquakes is the basis of typical microseismic imaging in the oil and gas industry.

In this paper, we review key microseismic monitoring projects with two objectives in mind. First, we review the development of the technology by looking backward in time at key developments and contributions from specific projects that were instrumental in developing the current application of the imaging technique. Second, we document the earliest application of the technology. Two alternative monitoring techniques are used today: surface and downhole monitoring. In downhole monitoring, high-sensitivity sensors are deployed in boreholes close to the seismic source to minimize signal attenuation and background noise. This detects small-magnitude microseismicity with signal-to-noise ratio (S/N) sufficient to determine source location from a sparse receiver array. A detection bias is introduced such that more small microseismic events are recorded close to the array and the ultimate detection range can be limited to a region around the monitoring location (e.g., Maxwell et al., 2006). Most hydraulic-fracturing imaging projects use offset observation wells, although borehole arrays can also be deployed in the treatment well itself (e.g., Gaucher et al., 2005) with associated increase in background noise resulting from the fluid being injected near the sensors.

Using downhole data, we determine locations of microseismic events using three general classes of techniques. The first class can be implemented with data from only one three-component (3-C) sensor and is generally called the hodogram technique (e.g., Albright and Hanold, 1976). In this method, the direction between the recording sensor and the microseismic location is determined from the particle motion of the direct P-wave and/or S-wave arrival, which under certain assumptions is polarized in the direction of propagation. The distance to the event is determined from the difference in arrival times between the direct P- and S-waves and knowledge of the P- and S-wave velocities. In the simplest implementation of the hodogram method, only one station is required, and the average velocities of the region are used. More reliable locations can be determined by hodograms from multiple recording locations and all available information about the velocity structure of the investigation region.

The second class of location approaches uses arrival times of combinations of P- and/or S-waves at multiple stations in a triangulation scheme (e.g., Gibowicz and Kijko, 1994). This and the previous class of location approaches can have spatially variable velocity information from the region of study. A third class of location methods involves finding the point in space that maximizes a semblance measure of the arrival of specific phases without the need for measuring the discrete arrival times (e.g., Drew et al., 2005; Rentsch et al., 2007). These semblance techniques can use a single phase, requiring a large aperture array, or multiple phases, more suited to smaller-aperture downhole arrays. This approach of source-location imaging is conceptually similar to Kirchhoff migration. In general, location approaches can combine hodogram and arrival-time information. The methodology used for a given microseismic study depends on the sensor configuration and the quality of the recorded data.

A clear assessment of the reliability of the location methodology is an important aspect of microseismic imaging to determine the scale of structures that can be resolved and to identify features that may be artifacts. Microseismic location accuracy is largely controlled by the geophone-array geometry and velocity model (Pavlis, 1986). Detailed local velocity information corresponding to horizontal travel paths from source to receiver is often unavailable; thus, downhole calibration shots are critical in providing accurate locations (Warpinski et al., 2005). Random errors affecting the relative scatter of locations are introduced primarily through traveltime picking uncertainty (e.g., Maxwell, 2010), which depends on S/N. Waveform correlation techniques can greatly reduce relative picking errors, improving the resolution of microseismic images (e.g., Phillips et al., 1997). Well surveys of the monitor wells are also important for accurate measure of receiver placement especially when wells are considered vertical (Bulant et al., 2007). With some a priori knowledge of velocity structure, downhole sensor configurations can be optimized within available wells to best detect and most accurately locate events within a volume of interest (e.g., Raymer et al., 2004).

As with natural earthquakes, other microseismic source characteristics can also be determined, such as magnitude or moment as a measure of the source strength and fault-plane solutions to determine fracture orientation and slip direction. More general source mechanisms to resolve volumetric or dilational components of deformation may be obtained, but they require sensors placed in multiple boreholes (Nolen-Hoeksema and Ruff, 2001; Vavryčuk, 2007) Finally, path effects associated with the transmission of the seismic waves can be analyzed and used to investigate rock properties, including measurements of shear-wave splitting or local microearthquake tomography for measuring velocity or attenuation changes affected by injection (Block et al. [1994] describe a geothermal example).

BARNETT SHALE HYDRAULIC-FRACTURE IMAGING

In 2000, the first successful hydraulic-fracture imaging project was completed in the Barnett Shale in the Fort Worth basin, Texas, U.S.A., using a wireline-deployed geophone array (Maxwell et al., 2002). At the time, the Barnett field was in the early phase of its development; it has since become one of the largest U. S. natural gas fields and has motivated an industry movement toward shale-gas development. The Barnett is a naturally fractured reservoir, and the injection of large volumes of water to stimulate the shale hydraulically results in a spatial distribution of the microseismic locations that is interpreted as occurring along the complex fracture network that is wide compared to the location uncertainty (see Figure 1). Although conventional hydraulic-fracture models assume that only a single fracture will be created, the complex fracture network found in formations such as the Barnett provide ongoing fracture engineering challenges because of the presence of multiple fractures having different orientations. Nevertheless, the microseismic images have proven valuable for optimizing production from wells in the Barnett.

Although initially skeptical, engineers began to accept the notion that the Barnett is naturally fractured, which led them to incorporate the concept of fracture complexity into the design of hydraulic fractures (Mayerhofer et al., 2006). Typically, hydraulic-fracture design is based on simplistic models of discrete hydraulic fractures. However, interaction of the fracture fluids with pre-existing fractures results in a complex fracture network as the injected fluid follows the path of least resistance that is determined locally by the fracture pattern and the local stress field. This fracture complexity means that the traditional hydraulic-fracture models are not appropriate. The engineering community is looking toward advanced tools (that include geomechanical effects) to account for deformation between the mechanically and hydraulically connected fracture network (e.g., Dusseault et al., 2007).

Nevertheless, a significant amount of engineering work has been initiated to better understand the microseismic imaging results in the Barnett. For example, studies show a correlation between production of Barnett wells and the volume of rock containing microseismicity (Mayerhofer et al., 2006) as well as the density of seismic moment as a measure of the density of the seismic deformation (Maxwell et al., 2006). Sensitivity studies using reservoir simulators based on conceptual fracture-network models derived from the microseismic images have been used to show the relation between production and both the volume of stimulated rock and the density of fractures (Mayerhofer et al., 2006).

The success of microseismic monitoring, along with the development of improved stimulation approaches and the optimization of horizontal wells, has made the Barnett the standard for shale-gas development. It is also the reservoir where microseismic studies are most often applied, with possibly thousands of hydraulic-fracture treatments monitored, representing about half of all microseismic hydraulic-fracture projects. Indeed, some field operators have begun to refer to microseismic monitoring in investor press releases. More importantly, the knowledge gained from microseismic studies in the Barnett is being applied to other tight-gas and shale-gas reservoirs, showing the importance of microseismic imaging.

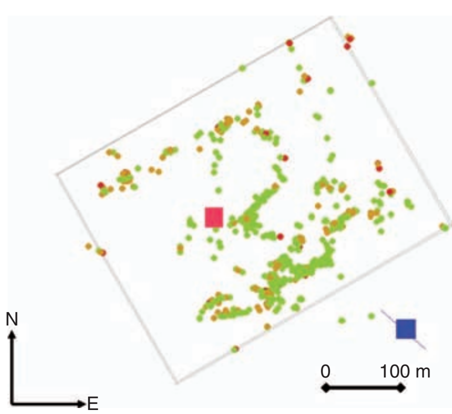

Figure 1. Map view of microseismicity recorded in 2000 during a hydraulic-fracture stimulation of the Barnett Shale. Blue square = monitoring well; red square = injection well. The microseismic symbols (circles) are color coded by moment magnitude (light green is < -1.9, orange is -1.9 to -1.5; red is > -1.5). The gray border represents a rectangular expression of the extent of the seismically active region. Contrast this apparent fracture complexity with the relatively simple fracture in Figure 2 (after Maxwell et al., 2002).

Currently, real-time microseismic imaging is being used in the Barnett to enhance production from new and old wells to optimize the fracture network as well as avoid fracturing into geohazards (Waters et al., 2009). One such hazard is fractures growing downward from the Barnett Shale into the underlying Ellenberger Limestone, after which the well can produce significant volumes of water. Real-time microseismic monitoring is the only viable technology available to engineers to avoid such geohazards. From the beginnings in the Barnett, microseismic monitoring of hydraulic fracturing has spread as an accepted and desired imaging technology, primarily in North American fields.

COTTON VALLEY SANDS HYDRAULIC-FRACTURE IMAGING

Although the commercial services focused on hydraulic-fracture imaging grew out of the Barnett Shale, the first Barnett work closely followed a comprehensive investigation of hydraulic fracturing in the tight-gas-sand reservoirs of the Piceance basin of northwestern Colorado (Warpinski et al., 1998a; Warpinski et al., 1998b; see references in both) and the Cotton Valley Sands of east Texas (Walker, 1997; Mayerhofer et al., 2000; Rutledge et al., 2004). The phased M-Site experiments in the Piceance basin, between 1983 and 1996, confirmed the validity of downhole microseismic-fracture mapping using single-wireline or permanently deployed borehole arrays and by coring through the microseismic cloud. In addition to hydraulic-fracture stimulations, microseismic mapping has been used to map hydraulic fractures created during drill-cutting injection. The ARCO waste injection project (Keck and Withers, 1994) into the Frio Formation is probably the first example of using a long, single-borehole array in a real field site. The Mounds experiment site, near Tulsa, Oklahoma, U.S.A., also includes coring through the fractures and confirmed the creation of multiple fracture planes as indicated by the microseismic images (Moschovodis et al., 2000).

Following the investigations at the M-Site, the Cotton Valley imaging project was conducted in 1997 (Walker, 1997). The monitoring tests were conducted in the Carthage gas field of east Texas using two instrumented boreholes to map and characterize various hydraulic fractures in tight gas sands. Designing the project benefited from the experience gained at M-Site and ARCO's waste-injection monitoring tests conducted a few years earlier. One objective of the Cotton Valley study was to establish whether differences between the responses of gel-proppant and waterfrac treatments (using water-based injection fluids instead of a viscous gel) could be gleaned from microseismic data. Earlier engineering studies indicated that waterfracs were just as effective as the more expensive gel-proppant treatments in the Cotton Valley Formation (Mayerhofer et al., 1997; Mayerhofer and Meehan, 1998).

Urbancic and Rutledge (2000) and Mayerhofer et al. (2000) present the initial processing and interpretation of the Cotton Valley data. Rutledge and Phillips (2003) and Rutledge et al. (2004) undertake a detailed investigation of the microseismicity induced by the two treatment types. Their analysis includes improving relative source locations, determining source mechanisms, and comparing the seismic moment released by the various injections. Interestingly, the seismicity induced by the two treatment types reveals nearly identical fracture geometries and mechanical responses for common stratigraphic intervals.

Figure 2 shows an example for injections into the top of the Cotton Valley formation. The gel-proppant and waterfrac treatments resulted in narrow zones of seismicity, 6–12 m wide. The gross fracture geometry is much simpler than that revealed in the Barnett Shale (Figures 1 and 2). Although the source locations of Figure 2 have been determined precisely, the original Cotton Valley locations as well as microseismic maps from other tight-gas-sand reservoirs (e.g., Warpinski et al., 1998b; Fischer et al., 2008) reveal fairly simple hydraulic-fracture geometries relative to the distributed multiple fracture branches resolved in the Barnett Shale (Figure 1). Treatment length for the Cotton Valley waterfrac appears to be about two-thirds of the length attained by the gel-proppant treatment, but the lengths scale proportionally to the injected volumes per unit length of borehole stimulated. In depth view, the seismicity forms distinct bands associated with the multiple perforated sand intervals that were treated simultaneously. The vertical containment within the sands was unexpected because stress contrasts are very small between the sands and shales of the Upper Cotton Valley.

The magnitude and mechanisms of seismic deformation induced by the two treatment types were also similar. The cumulative moment release per unit volume injected, a normalized measure of the seismically detected deformation, was identical for the two treatment types (Rutledge et al., 2004). Similar source mechanisms occurring over both treatment lengths are evident from waveform similarity for adjacent events and from nearly identical spatial patterns of P- and SH-wave polarities and amplitude ratios with respect to a common monitoring well (Figures 3 and 4). These mechanisms determined by Rutledge et al. (2004) were constrained to double-couple or shear sources (Figure 4), but a more general analysis of the moment tensors by Sileny et al. (2009) indicates significant non-double components of deformation accompany the shearing within the Cotton Valley. Finally, analyzing the time-space development of the seismic clouds, Dinske et al. (2009) also derive similar reservoir hydraulic properties and fracture dimensions (surface areas and width) from these two data sets.

The occurrence and banding of events in depth within the Cotton Valley appears to be associated with the reservoir's prevalent natural fractures, which are known to be isolated within the individual sands. Thus, the similar responses to the two treatment types in the Cotton Valley underscore how microseismicity is primarily generated and controlled by the natural fractures encountered or pressurized during stimulation.

The results of these early projects establish microseismicity as a viable imaging technology and help highlight the potential engineering and economic impact associated with a better understanding of the fracture geometry.

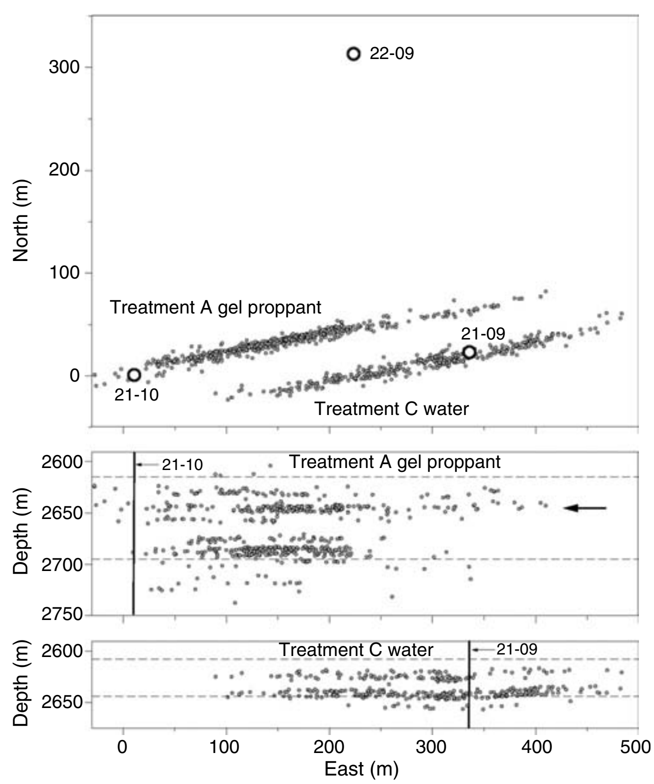

Figure 2. Source locations for gel-proppant (Treatment A) and waterfrac treatments (Treatment C) within the top of the Cotton Valley. The tops and bottoms of the perforated intervals are marked with the dashed lines in the depth views. The arrow marks one of the most populous depth-band clusters of treatment A. A subset of waveforms for events in that depth band is displayed in Figure 3 (after Rutledge et al., 2004).

CANADIAN STEAM-INJECTION RESERVOIR MONITORING

In 1997, Imperial Oil began to investigate the use of passive seismic monitoring to detect casing failures associated with thermal stress loading during cyclic steam stimulations (CSS) at Cold Lake, Alberta, Canada (Smith et al., 2002). Since that time, more than 100 well pads have been instrumented with microseismic monitoring systems.

In 2002, Shell Canada initiated an integrated monitoring program to image CSS, including microseismic monitoring (McGillivray, 2004). Microseismic imaging of CSS is conceptually similar to hydraulic-fracture imaging, in that comparable levels of seismicity are produced (Maxwell et al., 2003). Microseismic monitoring has also

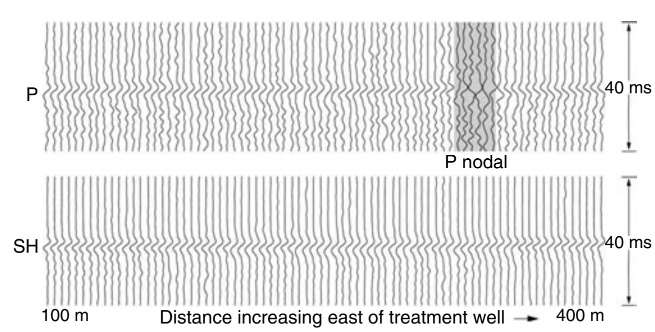

Figure 3. P- and SH-waveforms at one receiver in well 22-09. The corresponding sources are a subset of 78 higher-magnitude events within a 6-m depth interval marked by the arrow in Figure 2; they are sorted east to west over a range of 100–400 m from treatment well 21-10. The corresponding sources are not evenly spaced. Waveform character is very similar for adjacent sources, especially for the higher S/N SH-wave arrivals. The sense of P-first motions flip polarity over a short nodal interval near 265 m east. Each trace is scaled to its maximum amplitude and is windowed to align the arrival-time picks at 20 ms.

been performed to monitor the lower-pressure injections associated with steam-assisted gravity drainage techniques, resulting in lower levels of seismic deformation (Maxwell et al., 2008). Microseismic data, along with surface deformation and pressure data, were used to calibrate a coupled geomechanical reservoir model to optimize engineering of the injection (de Pater et al., 2008). Of all potential reservoir-monitoring applications of microseismicity, interpretation of steam-injection monitoring is the most common, with the significant levels of seismic deformation associated with the injections. Injections into other reservoirs at pressures below fracturing pressure and where thermal-related deformation is not expected are more challenging to interpret in terms of the relation between the fluid front and geomechanical deformation. Nevertheless, several past reservoir-monitoring projects show potential applications of the method.

YIBAL FIELD, OMAN, RESERVOIR MONITORING

Around the crest of the Yibal field in Oman, microseismic monitoring was conducted for about two years, during 2002 and 2003. The network consisted of eight-level strings of multicomponent geophones deployed in five abandoned wells. The geophone arrays spanned the shallower gas reservoir and extended to the underlying oil reservoir (Jones et al., 2004). The detailed positioning of the geophones was dependent on local factors such as cement quality. The wells were 1–2 km apart. About 7500 microseismic events were located and found to occur mostly along a specific subset of pre-existing faults. The monitoring was continuous; seismic activity varied considerably, spatially and temporally, and often was linked to reservoir operations such as the start of seasonal gas production. The gas reservoir is undergoing significant pressure depletion, and the oil reservoir is being waterflooded.

Microseismic activity is most intense within the shale sealing the gas reservoir. This has been interpreted as the result of differential compaction across the faults in the gas reservoir. Some groups of locations associated with the main structural faults extend downward 1 km toward the underlying oil reservoir (Bourne et al., 2006). The extended monitoring period reveals that some features remain seismically active over a prolonged period. This implies continuing deformation with time and represents a risk to wells because of the accumulating strain.

Focal mechanisms for a subset of events from a limited period of monitoring have been analyzed in detail; they show that a significant and systematic variation exists in the focal mechanisms for events located in the two different formations: reservoir rock or cap rock (Al-Anboori et al., 2006b). Frequency-dependent shear-wave splitting analysis was also carried out on a subset of the data (Al-Anboori et al., 2006a). The results indicate the reservoir rock has a much higher fracture density and typically larger fractures than the cap rock.

Further analysis of data from Oman has shown that results obtained from surface seismic observations are consistent with those obtained from analyzing downhole data, although the downhole data contain more small-magnitude events and delineate more details of the fracture pattern than could be obtained from five surface stations (Sarkar, 2008).

NORTH SEA RESERVOIR MONITORING

Microseismic activity was monitored in the Ekofisk field during April 1997 (Maxwell et al., 1998). Ekofisk is well known for its seafloor subsidence associated with reservoir compaction, and the microseismicity was investigated as a means to image fault structure

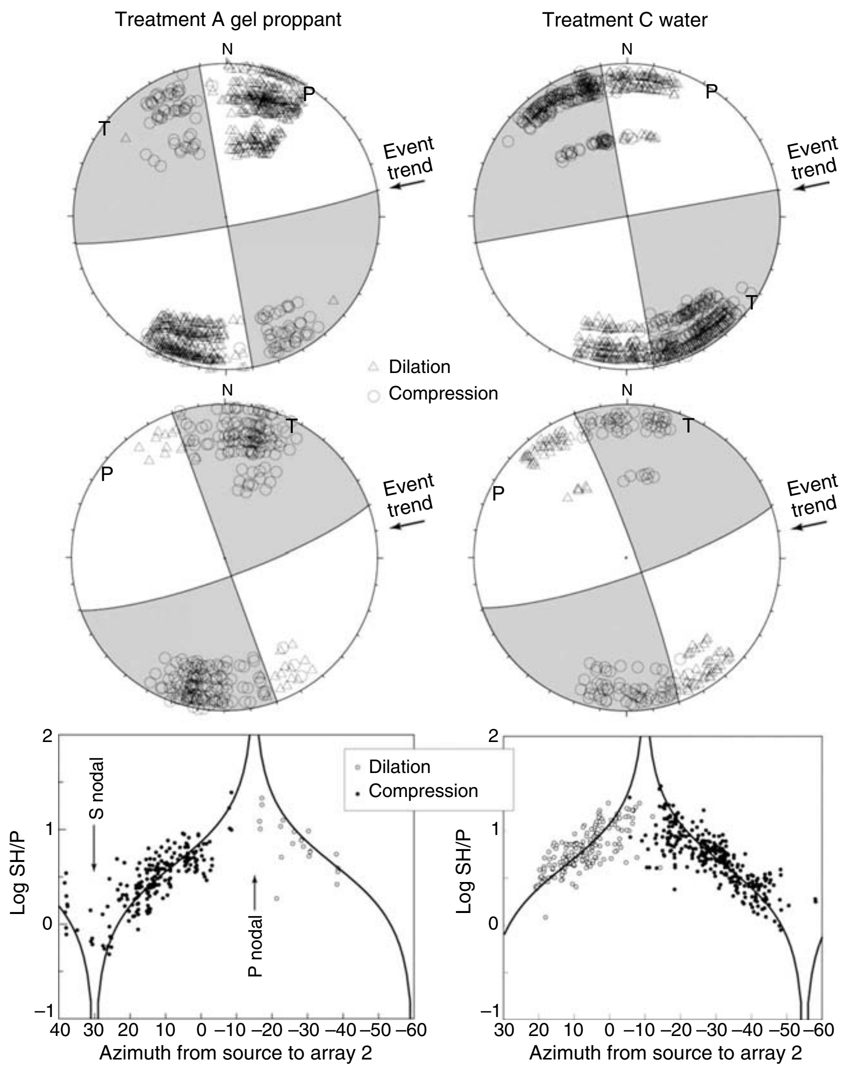

Figure 4. Composite focal mechanisms, constrained to double-couple solutions, for the treatments shown in Figure 2. At the bottom are composite plots of SH-/P-wave amplitude ratios versus azimuth from the sources back to receivers in well 22-09. The SH-/P-wave data correspond to the right and left lateral strike-slip solutions of the gel-proppant and waterfrac treatments, respectively. The P-wave polarities are also distinguished on the SH-/P-wave displays. The curves on the SH-/P-wave displays are the theoretical amplitude ratio for vertical strike-slip faults (see Rutledge and Phillips [2003] and Rutledge et al. [2004] for details).

under a gas cloud overlying the crest of the field. The monitoring was conducted using a six-level, 3-C wireline-deployed array in an observation well in the center of the field. A significant activity rate was observed, consistent with early monitoring at the site (Rutledge et al., 1994). The microseismic activity was concentrated within specific layers in the reservoir. The observed deformation was attributed to fault activation from the compaction, although interaction with a waterflood was also postulated (see Figure 5).

Following interest generated by the Ekofisk study, a similar monitoring was performed in the Valhall field in the Norwegian sector of the North Sea during summer 1998 (Dyer et al., 1999). The monitoring was again carried out using the same wireline tool deployed in a well near the crest of the field, which was awaiting workover. The monitoring period was 57 days. For operational reasons, the tool was deployed approximately 250 m shallower than had been originally intended. Modeling software demonstrated that the new deployment depth would still allow good coverage of the area of interest.

The event rate at Valhall ranged up to 10 events per day; 572 events were detected, of which 324 were located. A few shallow events were detected that could be directly related to sidetrack drilling activities taking place in a nearby well. All other events were located within a 50-m-thick zone above the Top Balder Formation reservoir. This corresponds to the depth interval where wellbore-stability problems were experienced (Kristiansen et al., 2000). Event locations showed two main structures, and analysis of the fault-plane solutions indicated a significant normal faulting component (Zoback and Zinke, 2002).

DeMeersman et al. (2009) have reprocessed the Valhall data using crosscorrelation and repicking to reduce location uncertainty and reveal greater structure. Locations within the main clusters correspond to faults mapped from 3D seismic. The time-varying nature of the shear-wave splitting reported by Teanby et al. (2004) is interpreted as resulting from cyclic stress changes in cap rock related to production-driven compaction of the reservoir. Zoback and Zinke (2002) analyze source mechanisms of fracture orientations and faulting mechanism at Ekofisk and Valhall.

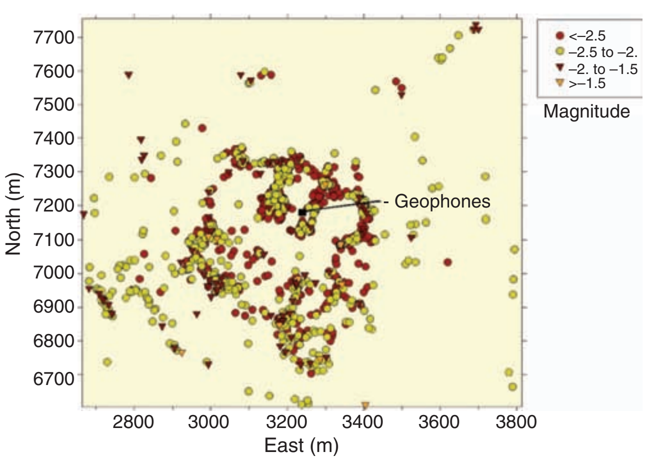

Figure 5. Map view of microseismicity recorded during April 1997 at Ekofisk, with colors defined by moment magnitude. The monitoring well is in the center. Microseismic deformation is attributed to compaction-related fault activation within the reservoir. See Maxwell et al. (1998) for details.

CLINTON COUNTY RESERVOIR MONITORING

One of the early studies demonstrating the capability to map productive reservoir fractures using downhole sensors was conducted in the Seventy-Six oil field of Clinton County, Kentucky, U.S.A. (Rutledge et al., 1998; Phillips et al., 2002). Oil is produced from low-porosity carbonate rocks at depths between about 300 and 730 m. The existence of isolated, high-volume wells in the area suggested the presence of isolated fractures with high permeability and storage capacity. However, the fracture orientations were generally unknown and were often assumed to be vertical. The monitoring tests involved deploying geophones near high-volume producing wells at several sites in Clinton County, with the goal of delineating the reservoir fracture system.

Figure 6 shows a perspective view of fracture planes revealed by the microseismicity, detected during a six-month period of monitoring. Approximately 1800 m^3 of oil was produced from well HT1 throughout that period, during which no injection operations were conducted. The microseismic locations and source mechanisms delineate a set of low-angle thrust faults that lie above and below the currently drained interval. These active fractures intersect or can be extrapolated to production intervals in the surrounding shut-in wells that produced oil in the nine months preceding monitoring. Two drilling tests into the main fracture produced brine (fracture A, Figure 6). Thus, the microseismic locations defined fractures that had contained oil but were drained and subsequently recovered to hydrostatic pressure via brine invasion. The identification and correlation of these faults with oil production indicated for the first time that these low-angle features should be considered important drilling targets in the exploration and development of the area.

This seismic behavior is consistent with poroelastic models that

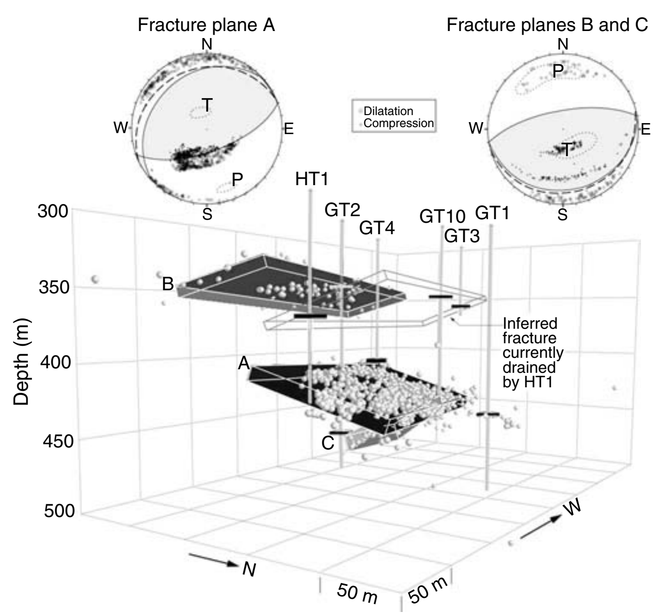

Figure 6. Perspective view of fracture planes defined by microseismic source locations in Clinton County, Kentucky, U.S.A. The fault-plane solutions displayed at the top indicate that the seismically active fractures are undergoing reverse or thrust faulting. The mechanisms were solved as composites by grouping the events from common planes. The dashed curves on the focal hemispheres represent the orientations of the planes determined from the respective source locations. See Rutledge et al. (1998) for details.

predict slight increases in horizontal stress above and below currently drained volumes. Alternatively, the change could be posed as crack closure from drainage, reducing the normal stress on the fractures above and below. Pressure re-equilibration via brine invasion replacing previously produced oil along the seismically active faults should also be weakly promoting the observed failure (Rutledge et al., 1998).

DISCUSSION

Prior to these specific projects, several microseismic projects were performed for various applications. Although there are too many examples to catalog all of these projects, here we focus on the earliest downhole microseismic monitoring examples known to the authors.

The earliest published example of computing a microseismic image of microseismic event locations solely from downhole monitoring is believed to be from a geothermal energy-related hydraulic fracture project at Fenton Hill in New Mexico, U.S.A. (Albright and Hanold, 1976). However, an earlier hydraulic fracture operation was mapped by El Paso Natural Gas Company in the San Juan basin in New Mexico in December 1973, followed by an expanded project in the Pinedale field in Wyoming in September 1974 (Power et al., 1976). Like the initial geothermal-energy related observations, the San Juan basin experiment used a single sensor but was able to identify microseismicity downhole attributed to the hydraulic fracture. The Pinedale monitoring used a combination of surface and downhole recording to generate a hydraulic-fracture image (Figure 7).

Even earlier investigations to develop the technology focused on recording signals to prove the occurrence of microseismicity, before imaging the source location of the microseismic events. Between 1967 and 1969, seismic monitoring was performed on hydraulic-fracture injections for waste disposal in a shale formation at the Oak Ridge National Laboratory in Tennessee, U.S.A. (McClain, 1971). Surface geophones were used to monitor the seismic deformation and initially involved analyzing characteristics of microseismic signals. A later phase of these experiments in 1970 involved a network of five sensors, used to create an epicentral map of the microseismic activity. In November 1972, microseismic waveforms were observed during a downhole recording of injection at the Wharton gas storage site in Pennsylvania (Hardy et al., 1975). Shuck (1974) reports microseismic waveforms recorded during a hydraulic fracture in Bradford, Pennsylvania, U.S.A., in July 1973. The development of downhole recording ultimately has been linked to challenges associated with the development of downhole sensors with enough sensitivity to record small ground motions of microseismic signals, as well as development of processing techniques to generate microseismic maps from single or multiple borehole-based sensors. Nevertheless, these pioneers shared the vision of the value of microseismic data that is finally being realized today.

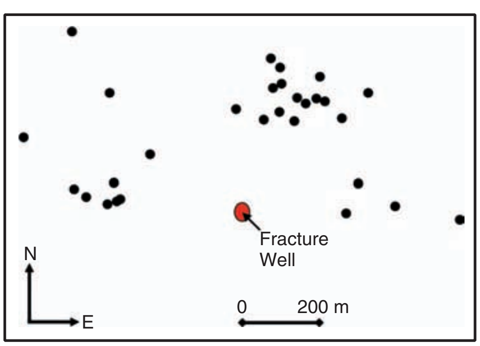

Figure 7. Map view of microseismicity recorded during a hydraulic fracture in Pinedale, Wyoming, U.S.A., in September 1974 (after Power et al., 1976).

Beyond this historical review of early microseismic efforts, it is interesting to note some of the comments in these early papers regarding challenges with the technology and future recommendations as perceived at the time. McClain (1971) recommends that development should continue to improve the reliability of the technique. Indeed, some of the ongoing issues with modern microseismic monitoring concerns understanding, quantifying, and improving the confidence and accuracy of the technique. Although all of these early papers discuss the drawbacks of S/N, which remains an issue today, Shuck (1974) also describes the problem of finding potential monitoring wells close enough to the injection well, an ongoing challenge for downhole microseismic monitoring projects.

CONCLUSION

In this paper, we have looked back in time at the development of modern microseismic monitoring. To conclude, we also would like to look forward at the challenges that the technique will face. Clearly, improved imaging will increase the accuracy and confidence of microseismic images. Instrumentation improvements, including the ability to place more sensors in wells to improve location accuracy and to enable source mechanism investigations along with improvements in S/N of acquired signals, will also expand the application of microseismic monitoring.

However, the greatest challenge is interpreting microseismic images, which represent the geomechanical response of the reservoir to injection. Hydraulic fracturing is relatively straightforward to interpret if the microseismicity occurs along fractures in response to the injection of fluids and the induced deformation that results from stress changes around the fracture. Integrating the microseismicity with other geophysical, geological, petrophysical, and geomechanical information improves the interpretation. Comparison of microseismic fracture geometries with reservoir characterization can help identify the relationship with the rock fabric and potentially identify well placement to optimize the fracture network. Improved identification of the conductive fracture network will ultimately allow better reservoir simulation and better understanding between the microseismic response and the ultimate production. However, a current challenge with the technology appears to be quantifying and assessing the accuracy and confidence of event locations to allow the interpreter to extract the appropriate details from the microseismic image. Low S/N can result in uncertain interpretation of the seismograms, and uncertainties in the velocity model used for processing can result in mislocations. Velocity heterogeneities and potential changes with time associated with injection or production are difficult to measure and are often ignored, so the associated location uncertainty typically is not estimated.

Quantifying and incorporating confidence and uncertainty in the interpretation requires cross-disciplinary communication between the geophysical practitioners, engineering interpreters, and end users. With the current level of commercial hydraulic-fracture projects and the relative simplicity of the geomechanics models, it is likely that these challenges will be engaged first in hydraulic fracturing and pave the way for more widespread use of microseismicity for reservoir monitoring.

REFERENCES

Al-Anboori, A., M. Kendall, and M. Chapman, 2006a, Fracture-induced frequency-dependent anisotropy, Yibal field, Oman: 68th Conference & Technical Exhibition, EAGE, Extended Abstracts, A047.

Al-Anboori, A., M. Kendall, D. Raymer, and R. Jones, 2006b, Spatial variations in microseismic focal mechanisms, Yibal field, Oman: 68th Conference & Technical Exhibition, EAGE, Extended Abstracts, A048.

Albright, J. N., and R. J. Hanold, 1976, Seismic mapping of hydraulic fractures made in basement rocks: Proceedings of the Energy Research and Development Administration (ERDA) Symposium on Enhanced Oil and Gas Recovery, vol. 2, Paper C-8.

Block, L., C. Cheng, M. Fehler, and W. S. Phillips, 1994, Seismic imaging of the velocity structure in the vicinity of a hydrofrac in a geothermal reservoir: Geophysics, **59**, 102–112.

Bourne, S. J., K. Maron, S. J. Oates, and G. Mueller, 2006, Monitoring reservoir deformation on land — Evidence for fault re-activation from microseismic, InSAR and GPS data: 68th Conference & Technical Exhibition, EAGE, Extended Abstracts, E026.

Bulant, P., L. Eisner, I. Psencik, and J. Le Calvez, 2007, Importance of borehole deviation surveys for monitoring of hydraulic fracturing treatments: Geophysical Prospecting, **55**, 891–899.

Collins, D. S., and R. P. Young, 2000, Lithological controls on seismicity in granite rocks: Bulletin of the Seismological Society of America, **90**, 709–723.

DeMeersman, K., J. M. Kendall, and M. van der Baan, 2009, The 1998 Valhall microseismic data set: An integrated study of relocated sources, seismic multiplets, and S-wave splitting: Geophysics, **74**, no. 5, B183–B195.

Denlinger, R. P., and C. G. Bufe, 1982, Reservoir conditions related to induced seismicity at The Geysers steam reservoir, northern California: Bulletin of the Seismological Society of America, **72**, 1317–1327.

de Pater, H., J. de Koning, S. Maxwell, and D. Walters, 2008, Geomechanics for interpreting SAGD monitoring using microseismicity and surface tiltmeters: International Thermal Operations and Heavy Oil Symposium, Society of Petroleum Engineers, Paper 117688.

Dinske, C., S. A. Shapiro, and J. T. Rutledge, 2009, Interpretation of microseismicity resulting from gel and water fracturing of tight gas reservoirs: Pure and Applied Geophysics.

Drew, J., D. Leslie, P. Armstrong, and G. Michaud, 2005, Automated microseismic event detection and location by continuous spatial mapping: Proceedings, Society of Petroleum Engineers Annual Technical Conference, Paper 95513.

Dusseault, M., S. Yin, L. Rothenburg, and H. Han, 2007, Seismic monitoring and geomechanics simulation: The Leading Edge, **26**, 610–620.

Dyer, B. C., R. H. Jones, J. F. Cowles, O. Barkved, and P. G. Folstad, 1999, Microseismic survey of a North Sea reservoir: World Oil, March, 74–78.

Eberhart-Phillips, D., and D. H. Oppenheimer, 1984, Induced seismicity in The Geysers geothermal area, California: Journal of Geophysical Research, **89**, no. B2, 1191–1207.

Fehler, M., 1989, Stress control of seismicity patterns observed during hydraulic fracturing experiments at the Fenton Hill Hot Dry Rock Geothermal Energy Site, New Mexico: International Journal of Rock Mechanics and Mining Sciences & Geomechanics Abstracts, **26**, no. 3–4, 211–219.

Fehler, M., and W. S. Phillips, 1991, Simultaneous inversion for Q and source parameters of microearthquakes accompanying hydraulic fracturing in granitic rock: Bulletin of the Seismological Society of America, **81**, 553–575.

Fischer, T., S. Hainzl, L. Eisner, S. A. Shapiro, and J. Le Calvez, 2008, Microseismic signatures of hydraulic fracture growth in sediment formations: Observations and modeling: Journal of Geophysical Research, **113**, no. B2, B02307.

Gaucher, E., C. Maisons, E. Fortier, and P. Kaiser, 2005, Fracture mapping using microseismic monitoring data recorded from treatment well — Results based on 20 hydro-fracturing jobs: 67th Conference & Technical Exhibition, EAGE, Extended Abstracts, C008.

Gibowicz, S. J., and A. Kijko, 1994, An introduction to mining seismology: Academic Press Inc.

Hardy, H. R., E. J. Kimble Jr., A. W. Khair, R. Y. Kim, G. L. Mowrey, J. W. Comeau, L. A. Beck, and M. V. Gopwani, 1975, Feasibility of utilizing microseismic techniques for the evaluation of underground gas storage reservoir stability: Pipeline Research Council International Inc. report L19725e, accessed 7 July 2010, http://www.prci.com/publicationsnew/L19725e.cfm.

Jones, R. H., D. Raymer, G. Mueller, H. Rynja, and K. Maron, 2004, Microseismic monitoring of the Yibal oilfield: 66th Conference & Technical Exhibition, EAGE, Extended Abstracts, A007.

Keck, R. G., and R. J. Withers, 1994, A field demonstration of hydraulic fracturing for solid waste injection with real-time passive seismic monitoring: Proceedings, Society of Petroleum Engineers Annual Technical Conference, Paper 28495.

Kristiansen, T., O. Barkved, and P. Patillo, 2000, Use of passive seismic monitoring in well and casing design in the compacting and subsiding Valhall field, North Sea: Proceedings, SPE European Petroleum Conference, Paper 65134.

Majer, E. L., and T. V. McEvilly, 1979, Seismological investigations at The Geysers geothermal field: Geophysics, **44**, 246–269.

Maxwell, S. C., 2010, Microseismic: Growth born from success: The Leading Edge, **29**, 338–343.

Maxwell, S. C., J. Du, and J. Shemeta, 2008, Passive seismic and surface monitoring of geomechanical deformation associated with steam injection: The Leading Edge, **27**, 260–266.

Maxwell, S. C., and T. Urbancic, 2001, The role of passive microseismic monitoring in the instrumented oil field: The Leading Edge, **20**, 636–639.

Maxwell, S. C., T. Urbancic, M. Prince, and C. Demerling, 2003, Passive imaging of seismic deformation associated with steam injection in western Canada: Proceedings, Society of Petroleum Engineers Annual Technical Conference, Paper 84572.

Maxwell, S. C., T. Urbancic, N. Steinsberger, and R. Zinno, 2002, Microseismic imaging of fracture complexity in the Barnett Shale: Proceedings, Society of Petroleum Engineers Annual Technical Conference, Paper 77440.

Maxwell, S. C., C. K. Waltman, N. R. Warpinski, M. J. Mayerhofer, and N. Boroumand, 2006, Imaging seismic deformation induced by hydraulic fracture complexity: Proceedings, Society of Petroleum Engineers Annual Technical Conference, Paper 102801.

Maxwell, S. C., R. P. Young, R. Bossu, A. Jupe, and J. Dangerfield, 1998, Microseismic logging of the Ekofisk reservoir: Proceedings, Eurock '98, Society of Petroleum Engineers/International Society for Rock Mechanics, Paper 47276.

Mayerhofer, M. J., E. P. Lolon, J. E. Youngblood, and J. R. Heinze, 2006, Integration of microseismic fracture mapping results with numerical fracture network production modeling in the Barnett Shale: Proceedings, Society of Petroleum Engineers Annual Technical Conference, Paper 102103.

Mayerhofer, M. J., and D. N. Meehan, 1998, Waterfracs — Results from 50 Cotton Valley wells: Proceedings, Society of Petroleum Engineers Annual Technical Conference, Paper 49104.

Mayerhofer, M. J., M. F. Richardson, R. N. Walker Jr., D. N. Meehan, M. W. Oehler, and R. R. Browning Jr., 1997, Proppants? We don't need no proppants: Proceedings, Society of Petroleum Engineers Annual Technical Conference, Paper 38611.

Mayerhofer, M. J., R. N. Walker Jr., T. Urbancic, and J. T. Rutledge, 2000, East Texas hydraulic fracture imaging project: Measuring hydraulic fracture growth of conventional sandfracs and waterfracs: Proceedings, Society of Petroleum Engineers Annual Technical Conference, Paper 63034.

McClain, W. C., 1971, Seismic mapping of hydraulic fractures: Oak Ridge National Laboratory report ORNL-TM-3502, accessed 7 July 2010, http:/www.ornl.gov/info/library/reports.shtml.

McGillivray, P. R., 2004, Microseismic and time-lapse monitoring of a heavy oil extraction process at Peace River: 74th Annual International Meeting, SEG, Expanded Abstracts, 572–575.

Moschovodis, Z., and the Mound Drill Cuttings Injection Field Experiment Executive Committee, 2000, The Mounds drill cuttings injection field experiment: Final results and conclusions: Proceedings, International Association of Drilling Contractors/Society of Petroleum Engineers (IADC/SPE) Drilling Conference, Paper 59115.

Nolen-Hoeksema, R. C., and L. J. Ruff, 2001, Moment tensor inversion of microseisms from the B-sand propped hydrofracture, M-site, Colorado: Tectonophysics, **336**, no. 1–4, 163–181.

Pavlis, G., 1986, Appraising earthquake hypocenter locations errors: A complete practical approach for single event locations: Bulletin of the Seismological Society of America, **76**, 1699–1717.

Pearson, C., 1981, The relationship between microseismicity and high pore pressure during hydraulic stimulation experiments in low permeability granite rock: Journal of Geophysical Research, **86**, no. B9, 7855–7864.

Phillips, W. S., L. S. House, and M. C. Fehler, 1997, Detailed joint structure in a geothermal reservoir from studies of induced microearthquake clusters: Journal of Geophysical Research, **102**, no. B6, 11745–11763.

Phillips, W. S., J. T. Rutledge, L. H. House, and M. C. Fehler, 2002, Induced microearthquake patterns in hydrocarbon and geothermal reservoirs: Six case studies: Pure and Applied Geophysics, **159**, no. 1, 345–369.

Pine, R. J., and A. S. Batchelor, 1984, Downward migration of shearing in jointed rock during hydraulic injections: International Journal of Rock Mechanics and Mining Sciences & Geomechanics Abstracts, **21**, no. 5, 249–263.

Power, D. V., C. L. Schuster, R. Hay, and J. Twombly, 1975, Detection of hydraulic fracture orientation and dimensions in cased wells: 50th Annual Fall Technical Conference & Exhibition, Society of Petroleum Engineers/American Institute of Mechanical Engineers, Paper SPE5626.

Rayleigh, C. B., J. H. Healy, and J. D. Bredehoeff, 1976, An experiment in earthquake control at Rangely Colorado: Science, **191**, 1230–1237.

Raymer, D., Y. Ji, R. Behrens, and J. Ricketts, 2004, Genetic algorithm design of microseismic injection-monitoring networks in the Tengiz field: 74th Annual International Meeting, SEG, Expanded Abstracts, 548–551.

Rentsch, S., S. Buske, S. Luth, and S. A. Shapiro, 2007, Fast location of seismicity: A migration-type approach with application to hydraulic-fracturing data: Geophysics, **72**, no. 1, S33–S40.

Rutledge, J. T., T. D. Fairbanks, J. N. Albright, R. R. Boade, J. Dangerfield, and J. H. Landa, 1994, Reservoir microseismicity at the Ekofisk oil field: Eurock '94 International Conference, International Society of Rock Mechanics/Society of Petroleum Engineers (ISRM/SPE).

Rutledge, J. T., and W. S. Phillips, 2003, Hydraulic stimulations of natural fracture as revealed by induced microearthquakes, Carthage Cotton Valley gas field, east Texas: Geophysics, **68**, 441–452.

Rutledge, J. T., W. S. Phillips, and M. J. Mayerhofer, 2004, Faulting induced by forced fluid injection and fluid flow forced by faulting: An interpretation of hydraulic-fracture microseismicity, Carthage Cotton Valley gas field, Texas: Bulletin of the Seismological Society of America, **94**, 1817–1830.

Rutledge, J. T., W. S. Phillips, and B. K. Schuessler, 1998, Reservoir characterization using oil-production-induced microseismicity, Clinton County, Kentucky: Tectonophysics, **289**, no. 1–3, 129–152.

Sarkar, S., 2008, Reservoir monitoring using induced seismicity at a petroleum field in Oman: Ph.D. dissertation, Massachusetts Institute of Technology.

Shuck, L. Z., 1974, The determination of direction and length of hydraulically induced fractures in petroleum reservoirs: A field experiment: Proceedings, Society of Petroleum Engineers Annual Technical Conference, Paper 5160.

Sileny, J., D. P. Hill, L. Eisner, and F. H. Cornet, 2009, Non-double-couple mechanisms of microearthquakes induced by hydraulic fracturing: Journal of Geophysical Research, **114**, no. B8, B08307.

Smith, R. J., N. S. Alinsangan, and S. Talebi, 2002, Microseismic response of well casing failures at a thermal heavy oil operation: Proceedings, Society of Petroleum Engineers/International Society for Rock Mechanics (SPE/ISRM) Conference, Paper 78203.

Suckale, J., 2010, Moderate-to-large seismicity induced by hydrocarbon production: The Leading Edge, **29**, 310–314.

Teanby, N., J. M. Kendall, R. Jones, and O. Barkved, 2004, Stress-induced temporal variations in seismic anisotropy observed in microseismic data: Geophysical Journal International, **156**, 459–466.

Urbancic, T. I., and J. Rutledge, 2000, Using microseismicity to map Cotton Valley hydraulic fracture: 70th Annual International Meeting, SEG, Expanded Abstracts, 1444–1448.

Vavryčuk, V., 2007, On the retrieval of moment tensors from borehole data: Geophysical Prospecting, **55**, no. 3, 381–391.

Walker, R. N. Jr., 1997, Cotton Valley hydraulic fracture imaging project: Proceedings, Society of Petroleum Engineers Annual Technical Conference, Paper 38577.

Warpinski, N. R., P. T. Branagan, R. E. Peterson, and S. L. Wolhart, 1998a, An interpretation of M-Site hydraulic fracture diagnostic results: Proceedings, Society of Petroleum Engineers Rocky Mountain Regional/Low Permeability Reservoirs Symposium, Paper 39950.

Warpinski, N. R., P. T. Branagan, R. E. Peterson, S. L. Wolhart, and J. E. Uhl, 1998b, Mapping hydraulic fracture growth and geometry using microseismic events detected by a wireline retrievable accelerometer array: Proceedings, Society of Petroleum Engineers Gas Technology Symposium, Paper 40014.

Warpinski, N. R., R. B. Sullivan, J. Uhl, C. Waltman, and S. Machovoe, 2005, Improved microseismic fracture mapping using perforation timing measurements for velocity calibration: Society of Petroleum Engineers Journal, **10**, no. 1, 14–23.

Waters, G., H. Ramakrishnan, J. Daniels, D. Bentley, J. Belhadi, and D. Sparkman, 2009, Unlocking the unconventional oil and gas reservoirs: Utilization of real time microseismic monitoring and hydraulic fracture diversion technology in the completion of Barnett Shale horizontal wells: Offshore Technology Conference, Paper 20268.

Zoback, M. D., and C. Zinke, 2002, Production-induced normal faulting in the Valhall and Ekofisk oil fields: Pure and Applied Geophysics, **159**, no. 1, 403–420.